Iterative Clipping for PAPR Reduction in Visible Light OFDM Communications

Zhenhua Yu[1,3], Robert J. Baxley[2] and G. Tong Zhou[1]
[1] School of Electrical and Computer Engineering, Georgia Institute of Technology, Atlanta, Georgia 30332–0250, USA
[2] Georgia Tech Research Institute, Atlanta, GA 30332-0821, USA
[3] Texas Instruments, 12500 TI Boulevard MS 8649, Dallas, TX 75243, USA
Email: zhenhuayu@gatech.edu

***Abstract*—Visible light communications (VLC) rely on white light emitting diodes (LEDs) to transmit information and provide illumination. White LEDs act as low pass filters and thus place a limitation on achievable data rates in VLC. Orthogonal frequency division multiplexing (OFDM) has been applied to VLC to best make use of the available modulation bandwidth through bit loading. However, VLC-OFDM waveforms exhibit high peak-to-average power ratio (PAPR). This drawback makes VLC-OFDM signals very sensitive to nonlinearity of LEDs and requires large biasing. We propose an iterative clipping method to reduce upper PAPR and lower PAPR of oversampled VLC-OFDM signals without introducing in-band distortions. Theoretical analysis of PAPRs distributions, and simulations of PAPR reduction scheme are presented in this paper.**

I. Introduction

Visible light communications (VLC) are motivated by more and more crowded radio frequency (RF) spectrum and fast growing solid-state lighting (SSL) technology [1], [2], [3]. VLC rely on white light emitting diodes (LEDs) to provide illumination and communication simultaneously. To achieve the goal of communication, simple and low-cost intensity modulation and direct detection (IM/DD) techniques are employed, thus only signal intensity information, not phase information, is modulated. White LEDs exhibit low pass filter characteristic [4]. To best make use of available bandwidth of LEDs and boost the achievable data rates, orthogonal frequency division multiplexing (OFDM) has been considered for VLC [5], [6], [7]. OFDM can support bit-loading technology, which allows allocating different numbers of bits to different subcarriers based on signal-to-noise power ratio (SNR) [8], [9]. IM/DD requires the electric signal to be real-valued and unipolar (positive-valued). To ensure that the OFDM time-domain signal is real-valued, Hermitian symmetry must be satisfied in the frequency-domain.

OFDM is known for its disadvantage of high peak-to-average power ratio (PAPR) [10] and thus is very sensitive to nonlinearity of LEDs [11]. Moreover, high PAPR requires large biasing to convert the bipolar OFDM signal into unipolar version [12], which makes the system optical power inefficient. Therefore, PAPR reduction is necessary in VLC-OFDM system. Although PAPR reduction is well studied in RF-OFDM communications [10], [13], there are some differences between RF-OFDM and VLC-OFDM to prevent directly applying conventional PAPR reduction methods to VLC-OFDM systems. First, RF-OFDM baseband signal is complex-valued and VLC-OFDM baseband signal is real-valued. Real-value OFDM signal has two PAPRs, namely upper PAPR and lower PAPR, and they are limited by asymmetric constraints in VLC. Second, in RF communicators, both in-band distortions and out-of-band power leakage should be taken into account in PAPR reduction schemes. However, in VLC-OFDM systems, because LED acts as a low-pass filter, the out-of-band subcarriers cannot be leveraged to transmit information to other users. Thus, we do not need to concern about the out-of-band interferences. This actually gives us more headroom to develop PAPR reduction schemes for VLC-OFDM systems.

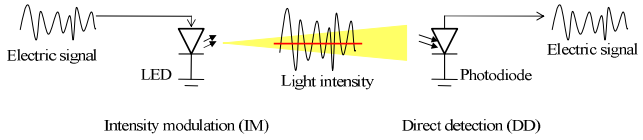

Fig. 1. Intensity modulation and direct detection in VLC

In this paper, we will first review VLC-OFDM systems and definitions of upper PAPR and lower PAPR. Then, we will extend the analysis of distributions of PAPRs for Nyquist-rate VLC-OFDM signals in reference [14] to oversampled VLC-OFDM signals. Next, the error vector magnitude (EVM) of clipped OFDM signals with bit loading will be investigated. Last, we will propose an iterative clipping method to reduce PAPRs of VLC-OFDM signals while ensuring no in-band distortions. The proposed PAPR reduction method is motivated by two clipping based PAPR reduction schemes proposed for RF-OFDM systems, namely, repeated clipping and filtering scheme [15], and constrained clipping scheme [16]. Rather than removing all out-of-band distortions to avoid adjacent channel interference as in [15], our proposed iterative clipping method eliminates all in-band distortions.

II. Dynamic Range Constrained Visible Light OFDM System

In VLC systems, intensity modulation (IM) is employed at the transmitter. The forward signal drives the LED which in turn converts the magnitude of the input electric signal into optical intensity. The human eye cannot perceive fast-changing variations of the light intensity, and only responds to the average light intensity. Direct detection (DD) is employed at the receiver. A photodiode (PD) transforms the received optical power into the amplitude of an electrical signal. Fig. 1 shows the basic concept of intensity modulation and direct detection in VLC.

978-1-4799-6770-4/14 $31.00 © 2014 IEEE
DOI 10.1109/MILCOM.2014.276

In an OFDM system, a discrete time-domain symbol sequence $\{x_n\}_{n=0}^{N-1}$ is generated by applying the inverse DFT (IDFT) operation to a frequency-domain sequence $\{X_k\}_{k=-N/2}^{N/2-1}$ as

$$\begin{aligned} x_n &= \text{IDFT}(X_k) \qquad (1) \\ &= \frac{1}{\sqrt{N}} \sum_{k=-N/2}^{N/2-1} X_k \exp\left(\frac{j2\pi kn}{N}\right), 0 \le n \le N-1, \end{aligned}$$

where $j = \sqrt{-1}$ and N is the size of IDFT. The resulting time-domain signals $\{x_n\}_{n=0}^{N-1}$ are complex-valued, including in-phase and quadrature components. However, in a VLC system using LED, IM/DD schemes require the electric signal to be real-valued. Thus, complex-valued OFDM in Eq. (1) cannot be used in VLC directly.

According to the property of the inverse Fourier transform, a real-valued time-domain signal x_n corresponds to a frequency-domain signal X_k that is Hermitian symmetric; i.e., $X_k = X_{-k}^*, 1 \le k \le N/2-1$, where $*$ denotes complex conjugate. The 0th and $-N/2$th subcarrier are null; i.e., $X_0 = 0$, $X_{-N/2} = 0$. Then we can obtain the real-valued time-domain signal Since the DC component is zero ($X_0 = 0$), x_n has zero mean and therefore is bipolar.

For visible light communications, the primary function is providing illumination. Thus, the LED has to emit white light, which includes the whole visible light spectrum from 375 to 780 nm (400 to 800 THz). Phosphorescent LED uses the blue LED chip coated with a yellow phosphor, which is the most popular white LED in the market due to its low cost. However, the slow response of phosphor limits the 3-dB modulation bandwidth of the phosphorescent white LEDS to only few MHz. A blue filtering can be operated at the receiver to increase the modulation bandwidth to 20 MHz. As an example, the frequency response of emitted white light and the blue part of a typical white light LED (Luxeon STAR) is shown in Fig. 2 [4]. It can be seen that white LED acts as a low-pass filter. OFDM enable the bit loading for each subcarrier to make the best use of the available modulation bandwidth. Generally, more bits are allocated to low-frequency subcarriers and fewer bit are allocated to high-frequency subcarriers. Let us define the in-band indices to be set $\mathcal{I} : [-N/2, N/2-1]$. Based on the number of bits loaded on each subcarrier, we divide the in-band subcarriers into a number of non-overlapped subsets; i.e., $\mathcal{I} = \mathcal{I}_1 \cup \mathcal{I}_2 \cup \cdots \cup \mathcal{I}_V$, where V is the number of subsets. Each subset of subcarriers are modulated by the same constellation type.

LEDs place dynamic range constraints $[I_L, I_H]$ on the input driving signals, where I_L denotes the minimum input current to turn on the LED, and I_H denotes the maximum input current to prevent overheating the LED. Since I_L is always a positive value, the original bipolar OFDM signal x_n has to be converted into unipolar (positive) signal. In this paper, we focus on the DC biased bipolar-to-unipolar conversion scheme, where the input signal of LEDs y_n is obtained via adding a biasing B to the original OFDM signal x_n; i.e.,

$$y_n = x_n + B. \qquad (2)$$

Adding a biasing will only affect the DC component X_0, which is not an issue since we do not put data on the DC subcarrier.

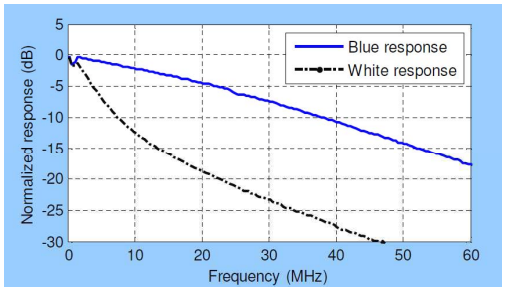

Fig. 2. Frequency response of emitted white light and the blue part of a typical white light (Luxeon STAR) LED [4].

III. PAPR IN VLC-OFDM

It is well-known that the OFDM time-domain signal has high peak-to-average power ratio (PAPR) , which is defined as

$$\text{PAPR} \triangleq \frac{\max\limits_{0 \le n \le N-1} |x[n]|^2}{\sigma_x^2}, \qquad (3)$$

where σ_x^2 is the variance of x_n. PAPR is a random variable and varies sequence by sequence. In the literature [10], the complementary cumulative distribution function (CCDF) is often used to quantify the distribution of PAPR. The CCDF of PAPR is defined as the probability that the PAPR exceeds a threshold r:

$$\text{CCDF}\{\text{PAPR}, r\} \triangleq Pr\{\text{PAPR} > r\} \qquad (4)$$

For the real-valued bipolar signal $\{x_n\}_{n=0}^{N-1}$, the square of the maximum value $\left(\max\limits_{0 \le n \le N-1} x_n\right)^2$ can be seen as the upper peak power, and the square of the minimum value $\left(\min\limits_{0 \le n \le N-1} x_n\right)^2$ can be seen as the lower peak power. In VLC, we previously demonstrated that the performance of OFDM is directly related with upper PAPR (UPAPR) and lower PAPR (LPAPR) [12], [14], [17], where the UPAPR of x_n is defined as $\mathcal{U}(x_n) \triangleq \left(\max\limits_{0 \le n \le N-1} x_n\right)^2 / \sigma_x^2$, and the LPAPR of x_n is defined as $\mathcal{L}(x_n) \triangleq \left(\min\limits_{0 \le n \le N-1} x_n\right)^2 / \sigma_x^2$.

Since Nyquist rate samples x_n might not represent the peaks of the continuous-time signal, it is desirable to show PAPR performance on oversampled discrete-time signals [15], [16]. It is shown that an oversampling ratio $L = 4$ is enough so that the PAPR before the digital to analog converter (DAC) can accurately describe the PAPR after the DAC [18]. It is typical to generate oversampled time-domain OFDM samples by zero-padding in the frequency domain [16]. Let us define the out-of-band indices to be the set $\mathcal{O} = [-NL/2, -N/2-1] \cup [N/2, LN/2-1]$, the zero padded version of X_k can be expressed as

$$X_k^{(L)} = \begin{cases} X_k, & k \in \mathcal{I} \\ 0, & k \in \mathcal{O} \end{cases}. \qquad (5)$$

An LN length IDFT is then applied to convert the frequency-domain sequence $\{X_k^{(L)}\}_{k=-LN/2}^{LN/2-1}$ into a L times oversampled

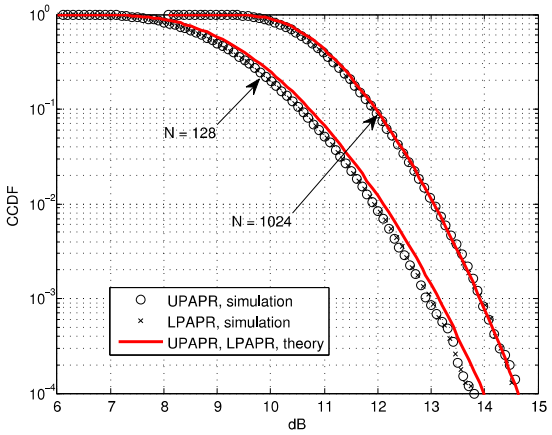

Fig. 3. CCDF of UPAPR and LPAPR of 4-times oversampled VLC-OFDM signals with $N = 128, 1024$.

TABLE I. BIT LOADING FOR DIFFERENT SUBCARRIERS SUBSETS ($N = 128$)

Subcarriers subset	Constellation type
$\mathcal{I}_1 = \{-21, \ldots, -2, -1\} \cup \{1, 2, \ldots, 21\}$	64-QAM
$\mathcal{I}_2 = \{-42, \ldots, -23, -22\} \cup \{22, 23, \ldots, 42\}$	16-QAM
$\mathcal{I}_3 = \{-63, \ldots, -44, -43\} \cup \{43, 44, \ldots, 63\}$	4-QAM

time-domain sequence $\{x_n^{(L)}\}_{n=0}^{LN-1}$. As a result of zero-padding in the frequency domain, the i.i.d. Gaussian assumption is not true for oversampled time-domain OFDM samples. The distribution of PAPR of L-times oversampled sequence can be approximated by αN-length i.i.d Gaussian sequence, where α is an empirical factor chosen to be $\alpha = 2.8$ [19]. Therefore, according to the derivations of Nyquist rate OFDM in [14], we can derive the individual and joint CCDFs of UPAPR and LPAPR for L-times oversampled OFDM signals as

$$\begin{aligned} \text{CCDF}\{\mathcal{U}(x_n^{(L)}), r_u\} &\triangleq Pr\{\mathcal{U}(x_n^{(L)}) > r_u\} \\ &= 1 - \Phi^{2.8N}(\sqrt{r_u}), \end{aligned} \tag{6}$$

$$\begin{aligned} \text{CCDF}\{\mathcal{L}(x_n^{(L)}), r_l\} &\triangleq Pr\{\mathcal{L}(x_n^{(L)}) > r_l\} \\ &= 1 - \Phi^{2.8N}(\sqrt{r_l}), \end{aligned} \tag{7}$$

$$\begin{aligned} &\text{CCDF}\{\mathcal{L}(x_n^{(L)}), \mathcal{U}(x_n^{(L)}), r_l, r_u\} \\ \triangleq\ & 1 - Pr\{\mathcal{L}(x_n^{(L)}) \le r_l, \mathcal{U}(x_n^{(L)}) \le r_u\} \\ =\ & 1 - [\Phi(\sqrt{r_u}) - \Phi(-\sqrt{r_l})]^{2.8N}. \end{aligned} \tag{8}$$

Fig. 3 shows the simulated CCDF of UPAPR and LPAPR of 4-times oversampled VLC-OFDM signals with $N = 128$ and 1024. The simulation results are drawn from 100000 OFDM sequences with bit-loading for different subcarriers set as shown in Table I and Table II. Theoretical results are plotted as well to examine our analysis. We can observe that the $\mathcal{U}$ and $\mathcal{L}$ are symmetrically distributed. When $N = 128$, slight differences can be found between the simulated results and the theoretical values. When $N = 1024$, the simulated results match the theoretical values very well because the central limit theory holds better.

TABLE II. BIT LOADING FOR DIFFERENT SUBCARRIERS SUBSETS ($N = 1024$)

Subcarriers subset	Constellation type
$\mathcal{I}_1 = \{-170, \ldots, -2, -1\} \cup \{1, 2, \ldots, 170\}$	64-QAM
$\mathcal{I}_2 = \{-340, \ldots, -172, -171\} \cup \{171, 172, \ldots, 340\}$	16-QAM
$\mathcal{I}_3 = \{-511, \ldots, -342, -341\} \cup \{341, 342, \ldots, 511\}$	4-QAM

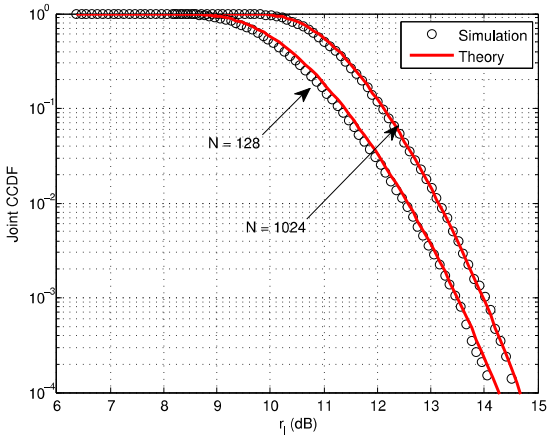

Fig. 4. Joint CCDF of UPAPR and LPAPR of 4-times oversampled VLC-OFDM signals with $\varrho = 0.5$ dB and $N = 128, 1024$.

According to Eq. (2), since the input signal of LEDS $y_n^{(L)}$ is constrained by the dynamic range $[I_L, I_H]$, the zero-mean OFDM signal before biasing $x_n^{(L)}$ is constrained by the dynamic range $[I_L - B, I_H - B]$. In VLC-OFDM, the biasing B is normally determined by the illumination level [17]. Therefore, although upper PAPR and lower PAPR are symmetrically distributed, they are not equally constrained, depending on where the OFDM signal is biased. We define the asymmetric factor as

$$\varrho \triangleq \frac{(I_H - B)^2}{(I_L - B)^2} \tag{9}$$

For example, $\varrho = 1$ dB means the upper PAPR is 1 dB less constrained than the lower PAPR. Thus, the UPAPR threshold r_u and the LPAPR threshold r_l have the relationship $r_u = \varrho r_l$. It is useful to know the joint CCDF with asymmetric factor ρ

$$\begin{aligned} &\text{CCDF}\{\mathcal{L}(x_n^{(L)}), \mathcal{U}(x_n^{(L)}), r_l, \rho r_l\} \\ =\ & 1 - [\Phi(\sqrt{\varrho r_l}) - \Phi(-\sqrt{r_l})]^{2.8N}. \end{aligned} \tag{10}$$

Fig. 4 shows the joint CCDF of UPAPR and LPAPR of 4-times oversampled VLC-OFDM signals with $\varrho = 0.5$ dB and $N = 128, 1024$. It can be seen that the simulated results match the theoretical values very well.

IV. PAPR REDUCTION

A. Simple clipping

Clipping is the simplest way to reduce the PAPR of OFDM signals. Given the oversampled real-valued OFDM signals $x_n^{(L)}$, the clipped version $\bar{x}_n^{(L)}$ is given by

$$\bar{x}_n^{(L)} = \begin{cases} c_u, & x_n^{(L)} > c_u \\ x_n^{(L)}, & c_l \le x_n^{(L)} \le c_u \\ c_l, & x_n^{(L)} < c_l \end{cases} \tag{11}$$

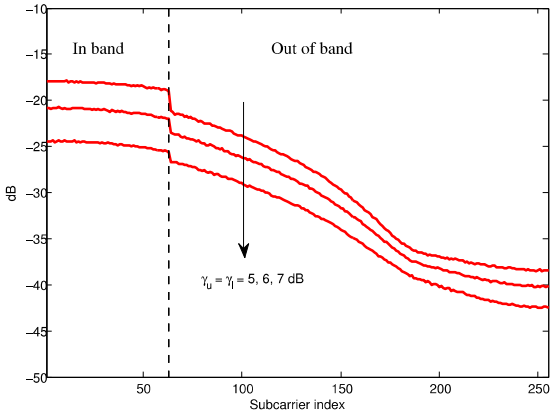

Fig. 5. Average power of clipping distortions on each subcarrier with $\gamma_u = \gamma_l = 5, 6, 7$ dB.

where c_u denotes upper clipping level and c_l denotes lower clipping level, respectively. Let us define the upper clipping ratio $\gamma_u \triangleq c_u^2/\sigma_x^2$, and lower clipping ratio $\gamma_l \triangleq c_l^2/\sigma_x^2$. The clipped signals can be expressed as the original signals plus distortions $d_n^{(L)}$; i.e.,

$$\bar{x}_n^{(L)} = x_n^{(L)} + d_n^{(L)}. \tag{12}$$

Taking DFT of both sides of Eq. (12), the clipped signals in the frequency domain are obtained as

$$\begin{aligned} \bar{X}_k^{(L)} &= X_k^{(L)} + D_k^{(L)} \\ &= \begin{cases} X_k + D_k^{(L)}, & k \in \mathcal{I} \\ D_k^{(L)}, & k \in \mathcal{O} \end{cases}, \end{aligned} \tag{13}$$

where $D_k^{(L)}$ denotes the distortion on the kth subcarrier. Fig. 5 shows the average power of distortions on each subcarrier $E\{|D_k^{(L)}|^2\}$ with different upper and lower clipping ratios. The bits are allocated according to the Table I. It can be seen that clipping distortions spread over both in-band and out-of-band subcarriers, and are almost equally distributed on in-band subcarriers. Because LEDs act as a low pass filter, we assume that the out-of-band subcarriers are not leveraged by other users. In other words, the out-of-band power leakage is not an issue in VLC. Thus, we only concern about in-band distortions. Error vector magnitude (EVM) is a widely used figure of merit in literatures [7], [20] and standards to quantify the in-band distortions, which is defined as

$$\text{EVM} \triangleq \sqrt{\frac{\sum_{k\in\mathcal{I}} E\{|D_k^{(L)}|^2\}}{\sum_{k\in\mathcal{I}} E\{|X_k^{(L)}|^2\}}}. \tag{14}$$

To ensure reliable communication, the EVM of transmitted signals should be below some threshold. As we know, high order constellations are more sensitive to noises than lower order constellations. In LTE [21], the EVM thresholds are 17.5% (4-QAM), 12.5% (16-QAM), and 8.0% (64-QAM), respectively. Thus, it is necessary for us to examine the constellation-wise EVM for a specific subcarriers subset $\mathcal{I}_v$

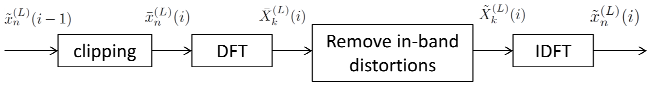

Fig. 7. Structure of iterative clipping scheme for each iteration.

, which is defined as

$$\text{EVM}_{\mathcal{I}_v} \triangleq \sqrt{\frac{\sum_{k\in\mathcal{I}_v} E\{|D_k^{(L)}|^2\}}{\sum_{k\in\mathcal{I}_v} E\{|X_k^{(L)}|^2\}}}. \tag{15}$$

As an example, Fig. 6 shows the corrupted constellations after clipping for different subcarriers subsets (constellation types) and their corresponding constellation-wise EVMs, where the constellations are arranged according to Table I and the clipping ratios are chosen as $\gamma_u = \gamma_l = 6$ dB. While the EVM for 64-QAM have violates the requirement 8.0%, there are still some room for 4-QAM and 16-QAM constellations. However, simpling clipping scheme is not able to control the distributions of distortions. The clipping ratios must be selected to satisfy the minimum EVM requirement among all the modulation types.

B. Proposed iterative clipping

Reducing PAPR of VLC-OFDM signals via clipping is straightforward and efficient, but at the same time introduces in-band distortions. The amount of clipping must be controlled wisely, to satisfy constellation-wise EVM constraints. In this section, we propose an iterative clipping method to reduce PAPR of VLC-OFDM signals while ensuring no in-band distortions. Due to the asymmetric constraints on upper PAPR and lower PAPR as in (9), the goal is actually to reduce the metric $J \triangleq \max\{\mathcal{U}, \varrho\mathcal{L}\}$. Therefore, the upper clipping level c_u is related with lower clipping level c_l as $c_u = -\sqrt{\varrho}c_l$.

Fig. 7 shows the overall structure of the proposed iterative clipping scheme for each iteration. Let $\tilde{x}_n^{(L)}(i-1)$ denote the output from the $(i-1)$th iteration, which serves as the input of ith iteration. For initial case $i = 0$, we let $\tilde{x}_n^{(L)}(0) = x_n^{(L)}$. In the ith iteration, $\tilde{x}_n^{(L)}(i-1)$ is double side clipped at upper clipping level c_u and lower clipping level c_l:

$$\bar{x}_n^{(L)}(i) = \begin{cases} c_u, & \tilde{x}_n^{(L)}(i-1) > c_u \\ \tilde{x}_n^{(L)}(i-1), & c_l \le \tilde{x}_n^{(L)}(i-1) \le c_u \\ c_l, & \tilde{x}_n^{(L)}(i-1) < c_l \end{cases} \tag{16}$$

Next, the clipped signal $\bar{x}_n^{(L)}(i)$ is transformed to the frequency domain with an LN-point DFT which outputs the signal as

$$\bar{X}_k^{(L)}(i) = \text{DFT}\{\bar{x}_n^{(L)}(i)\}, k \in \mathcal{I} \cup \mathcal{O} \tag{17}$$

Third, we set all the in-band subcarriers to the original constellations and leave all the out-of-band subcarriers unchanged to generate $\tilde{X}_k^{(L)}(i)$ as

$$\tilde{X}_k^{(L)}(i) = \begin{cases} X_k^{(L)}, & k \in \mathcal{I} \\ \bar{X}_k^{(L)}(i), & k \in \mathcal{O} \end{cases}, \tag{18}$$

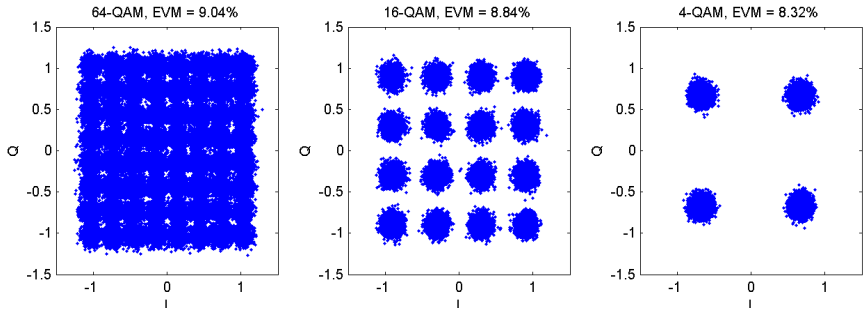

Fig. 6. Corrupted constellations and EVM with $\gamma_u = \gamma_l = 6$ dB.

This operation eliminates all the in-band distortions.

Last, the time-domain signals $\tilde{x}_n^{(L)}(i)$ are created with an LN-point inverse DFT operation

$$\tilde{x}_n^{(L)}(i) = \text{IDFT}\{\tilde{X}_k^{(L)}(i)\} \tag{19}$$

Note that since the DC component $\tilde{X}_0^{(L)}(i) = X_0^{(L)} = 0$, $\tilde{x}_n^{(L)}(i)$ is zero mean. Then we calculate the objective metric

$$J(i) = \max\{\mathcal{U}(\tilde{x}_n^{(L)}(i)), \varrho\mathcal{L}(\tilde{x}_n^{(L)}(i))\}, \tag{20}$$

and compare with the lowest metric $J_{\min}$ of previous $i-1$ iterations. If $J(i) < J_{\min}$, we set $J_{\min} = J(i)$ and store the output $\hat{x}_n^{(L)} = \tilde{x}_n^{(L)}(i)$.

If i has reached the maximum iteration number M, we obtain the final low-PAPR signals $\hat{x}_n^{(L)}$; otherwise, go to the $(i+1)$th iteration.

For the purpose of simulation, we generated 100000 VLC-OFDM symbols according to the parameters in Table I. We assumed that the asymmetric factor ϱ is 0.5 dB. We chose $\gamma_l = 7$ dB, and $\gamma_u = 7.5$ dB. Fig. 8 compares the joint CCDF of PAPRs of original VLC-OFDM signals with VLC-OFDM signals after various numbers of iterations. It can be seen that more iterations result in better PAPR reduction performance. Fig. 9 plots the joint CCDF of VLC-OFDM signals after 50 iterations with various clipping ratios. We can observe that smaller clipping ratios lead to better PAPR reduction performance when PAPR threshold is less than 8 dB. For PAPR threshold greater than 8 dB, higher clipping ratios achieve slightly better performance. Fig. 10 plots the corresponding average power of distortions in the frequency domain. We can see that all the clipping noises fall on out-of-band subcarriers. Out-of-band noises can be simply dropped at the receiver without any information loss. Moreover, because LED is a low-pass filter, the out-of-band subcarriers cannot be used to transmit information to other users reliably, and thus we do not need to concern about the interference with other users in VLC.

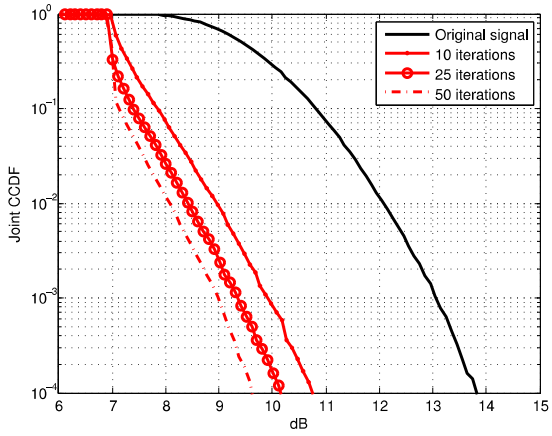

Fig. 8. Joint CCDF of PAPRs of VLC-OFDM signals after various numbers of iterations.

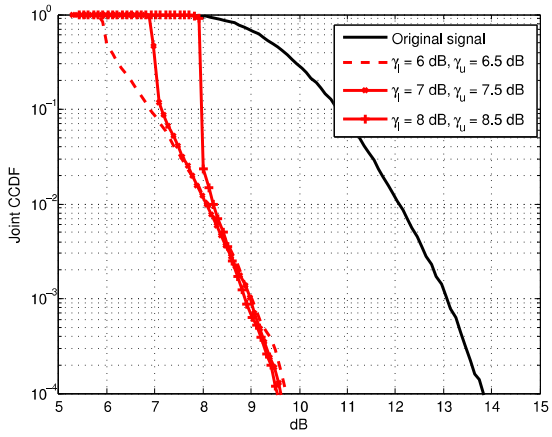

Fig. 9. Joint CCDF of PAPRs of VLC-OFDM signals after 50 iterations with various clipping ratios.

V. Conclusion

In this paper, we analyzed the distributions of PAPRs of oversampled OFDM signals in visible light communications. We reviewed dynamic range constraints and discussed motivations for PAPR reduction in VLC-OFDM. Clipping is the simplest way to achieve PAPR reduction, but generates in-band distortions. We found that clipping distortions are almost uniformly distributed among in-band subcarriers, which makes high order constellations vulnerable to clipping noises. To reduce the PAPRs of VLC-OFDM signals, an iterative clipping method was proposed without introducing in-band distortions. Simulation results shows that more than 4 dB PAPR reduction can be achieved after 50 iterations.

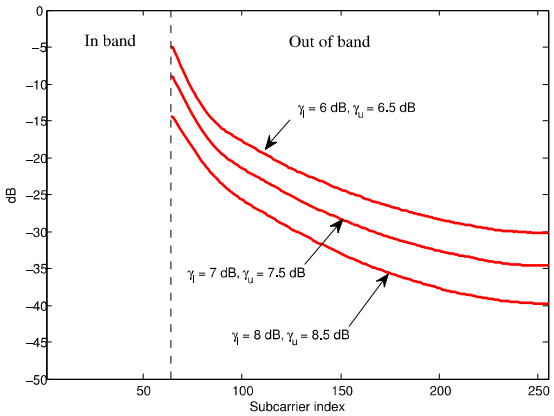

Fig. 10. Average power of clipping distortions on each subcarrier after 50 iterations with various clipping ratios.

ACKNOWLEDGMENT

This research was supported in part by the Texas Instruments Leadership University Program and in party by the National Science Foundation under grant no. ECCS-1343256.

REFERENCES

[1] D. O'Brien, L. Zeng, H. Le-Minh, G. Faulkner, J. W. Walewski, and S. Randel, "Visible light communications: Challenges and possibilities," in *Proc. IEEE 19th International Symposium on Personal, Indoor and Mobile Radio Communications*. IEEE, 2008, pp. 1–5.

[2] H. Elgala, R. Mesleh, and H. Haas, "Indoor optical wireless communication: potential and state-of-the-art," *IEEE Communications Magazine*, vol. 49, no. 9, pp. 56–62, 2011.

[3] Z. Yu, R. J. Baxley, and G. T. Zhou, "Multi-user MISO broadcasting for indoor visible light communication," in *IEEE International Conference on Acoustics, Speech and Signal Processing*, Vancouver, Canada, May 2013, pp. 4849–4853.

[4] H. L. Minh, D. O. Brien, G. Faulkner, L. Zeng, K. Lee, and D. Jung, "100-Mb/s NRZ Visible Light Communications Using a Postequalized White LED," *IEEE Photonics Technology Letters*, vol. 21, no. 15, pp. 1063–1065, 2009.

[5] S. Hranilovic, "On the design of bandwidth efficient signalling for indoor wireless optical channels," *International Journal of Communication Systems*, vol. 18, no. 3, pp. 205–228, 2005.

[6] J. Armstrong, "OFDM for optical communications," *Journal of Lightwave Technology*, vol. 27, no. 3, pp. 189–204, 2009.

[7] Z. Yu, R. J. Baxley, and G. T. Zhou, "EVM and achievable data rate analysis of clipped OFDM signals in visible light communication," *EURASIP Journal on Wireless Communications and Networking*, vol. 2012, Oct. 2012.

[8] A. M. Khalid, G. Cossu, R. Corsini, P. Choudhury, and E. Ciaramella, "1-Gb/s Transmission Over a Phosphorescent White LED by Using Rate-Adaptive Discrete Multitone Modulation," *IEEE Photonics Journal*, vol. 4, no. 5, pp. 1465–1473, Oct. 2012.

[9] D. Tsonev, H. Chun, S. Rajbhandari, J. McKendry, S. Videv, E. Gu, M. Haji, S. Watson, A. Kelly, G. Faulkner, M. Dawson, H. Haas, and D. O'Brien, "A 3-Gb/s Single-LED OFDM-based Wireless VLC Link Using a Gallium Nitride μLED," *Photonics Technology Letters, IEEE*, vol. PP, no. 99, p. 1, 2014.

[10] R. J. Baxley and G. T. Zhou, "Peak-to-Average Power Ratio Reduction," in *Digital Signal Processing Handbook*, 2nd ed., V. Madisetti, Ed. CRC Press, 2009.

[11] R. Mesleh, H. Elgala, and H. Haas, "LED Nonlinearity Mitigation Techniques in Optical Wireless OFDM Communication Systems," *Journal of Optical Communications and Networking*, vol. 4, no. 11, p. 865, Oct. 2012.

[12] Z. Yu, R. J. Baxley, and G. T. Zhou, "Peak-to-Average Power Ratio and Illumination-to-Communication Efficiency Considerations in Visible Light OFDM Systems," in *IEEE Intl. Conference on Acoustics, Speech, and Signal Processing*, Vancouver, Canada, 2013.

[13] ——, "Generalized interior-point method for constrained peak power minimization of OFDM signals," in *2011 IEEE International Conference on Acoustics, Speech and Signal Processing (ICASSP)*. Prague, Czech Republic: IEEE, May 2011, pp. 3572–3575.

[14] ——, "Distributions of upper PAPR and lower PAPR of OFDM signals in visible light communications," in *IEEE Intl. Conference on Acoustics, Speech, and Signal Processing*, Florence, Italy, 2014.

[15] J. Armstrong, "Peak-to-average power reduction for OFDM by repeated clipping and frequency domain filtering," *Electronics Letters*, vol. 38, no. 5, p. 246, Feb. 2002.

[16] R. J. Baxley, C. Zhao, and G. T. Zhou, "Constrained Clipping for Crest Factor Reduction in OFDM," *IEEE Transactions on Broadcasting*, vol. 52, no. 4, pp. 570–575, Dec. 2006.

[17] Z. Yu, R. J. Baxley, and G. T. Zhou, "Brightness Control in Dynamic Range Constrained Visible Light OFDM Systems," in *IEEE WOCC*, Newark, NJ, Mar. 2014.

[18] M. Sharif and B. Khalaj, "Peak to mean envelope power ratio of oversampled OFDM signals: an analytical approach," *IEEE International Conference on Communications*, pp. 1476–1480, 2001.

[19] R. van Nee and A. de Wild, "Reducing the peak-to-average power ratio of OFDM," in *IEEE VTC*, 1998, pp. 2072–2076.

[20] S. Kowlgi, P. Mattheijssen, C. Berland, and T. Ridgers, "EVM considerations for convergent multi-standard cellular base-station transmitters," *2011 IEEE 22nd International Symposium on Personal, Indoor and Mobile Radio Communications*, no. 1, pp. 1865–1869, Sep. 2011.

[21] D. Astely, E. Dahlman, A. Furuskar, Y. Jading, M. Lindstrom, and S. Parkvall, "LTE: the evolution of mobile broadband," *IEEE Communications Magazine*, vol. 47, no. 4, pp. 44–51, Apr. 2009.